

Cyclic fatigue of high strength optical fibers in bending

M. John Matthewson^a and Vishal Padiyar^b

Rutgers, The State University of New Jersey, Piscataway, NJ 08854

^aDepartment of Ceramic and Materials Engineering

^bDepartment of Electrical and Computer Engineering

ABSTRACT

Optical fiber may experience cyclic stresses at frequencies ranging from a few hertz in aerial cables to over a kilohertz due to vibration of machinery. The fatigue behavior of brittle materials typically gives times to failure that correspond to a suitably time-averaged applied stress and is independent of the frequency. Previous studies have been limited in the frequencies used but generally show agreement with this simple model. In this paper we describe results for the cyclic fatigue behavior of high strength fused silica optical fibers as a function of stress amplitude and frequency in the range of zero to 100 Hz. The results confirm that fatigue of this material is indeed accurately described by the subcritical crack growth model and the results are shown to be frequency independent in the range studied.

Keywords: Optical fiber, strength, fatigue, reliability, cyclic fatigue, stress corrosion

1. INTRODUCTION

For the purposes of making reliability estimates for optical fibers, the service stress is usually modeled as a static stress. However, in many applications the fiber might also be subjected to a cyclic component of stress superimposed on the static component. The cyclic stress can occur over a broad range in frequency; for example, ~10 Hz due to turbulent airflow past aerial cables, ~100 Hz from road traffic noise, and ~1 kHz and above in vibrating machinery. It is therefore important to understand the impact of cyclic stresses on optical fiber reliability.

It is well known that cyclic stresses produce crack growth in metals and polymers due to plastic processes at or near the crack tip. More recently it has been recognized that some polycrystalline ceramics can also exhibit cyclic fatigue by mechanisms that are not always clear.¹ One mechanism that has been identified in highly tough ceramics is wear of crack bridges by repeated rubbing. A characteristic of cyclic fatigue is that the fatigue rate depends more strongly on the stress amplitude than on the mean stress. Damage is introduced on each stress cycle and so the failure criterion is one of cycles to failure – the time to failure therefore directly depends on the cyclic frequency. However, it is usually thought that brittle materials do not exhibit cyclic fatigue though failure still occurs by stress corrosion cracking. The time to failure therefore depends on a suitable time average of the stress and has no dependence on the frequency. As a result of the anticipated lack of a cyclic fatigue effect, there have been few studies of cyclic fatigue in glasses.

Evans and Fuller² have determined how the time to failure under cyclic fatigue should depend on the mean stress and stress amplitude if the only process occurring during cyclic fatigue is subcritical crack growth. Comparison of experiment with their theory and the dependence of time to failure on frequency can be used to determine if any cyclic effects are occurring over and above subcritical crack growth. Evans and Fuller² compared their theory to the limited published experimental data for bulk glass but the results were inconclusive due to the large scatter in the measurements. They did, however, find that slow crack growth data for glass and porcelain is primarily due to stress corrosion. Evans and Linzer³ found no cyclic effects for crack propagation in glass up to a frequency of 600 Hz. Dill *et al.*⁴ did observe cyclic effects in slow crack growth in borosilicate glass. However, strength and static fatigue measurements of bulk glass specimens generally have too much scatter to provide a sensitive enough test for cyclic effects. Optical fibers in short lengths have very much lower scatter in their mechanical properties and so provide a better opportunity for detecting any cyclic effects.

Wysocki *et al.*⁵ applied cyclic stress to aluminum coated fiber and found that failure of the fiber only occurred after failure of the aluminum by metal fatigue. Rogers⁶ attached optical fibers to a crank to simulate a fiber sensor attached to the piston in an internal combustion engine. The fibers were flexed at 28.8 Hz under relatively low stress. Polyimide and acrylate coated fibers did not fail after an hour, as would be expected for subcritical crack growth. However, aluminum coated fibers failed in minutes due to fatigue of the metal coating. This shows that, while cyclic effects in glass might not be a concern for reliability, other components in a fiber or cable structure might well accelerate failure of the fiber. Katsuyama *et al.*⁷ found no deviation from the Evans and Fuller model² for cyclic fatigue of silicone/nylon coated fibers at low frequency (~0.007 to

0.07 Hz) and for relatively short times to failure (≤ 1000 s, *i.e.* ≤ 70 cycles to failure). Mauron *et al.*⁸ studied fiber Bragg gratings in tension under cyclic fatigue at 4 Hz and found no cyclic effects. In other work, they did observe cracking of a polyimide coating under cyclic conditions.⁹ Roneree *et al.*¹⁰ presented preliminary results for cyclic fatigue of high strength fiber in two-point bending at frequencies up to 100 Hz and also found no evidence of cyclic effects. While it appears from the previous work on fused silica optical fiber that there is no cyclic fatigue effect in the glass, other than the effect of subcritical crack growth, published studies are limited and have not explored a broad range of frequency or stress amplitude and so do not provide a sensitive test for cyclic effects. We present here results for cyclic fatigue in two-point bending at frequencies from zero to 100 Hz.

2. THEORY

Evans and Fuller² used the subcritical crack growth model to predict how the time to failure under cyclic conditions depends on the mean applied stress and stress amplitude. They showed that, under certain restrictions, the time to failure under cyclic conditions, t_f^{cyclic} , could be expressed in closed form:

$$\frac{t_f^{static}}{t_f^{cyclic}} = \sum_{i=0}^{(n \text{ div } 2)} \left(\frac{n!}{(n-2i)!(i!)^2} \right) \left(\frac{\zeta}{2} \right)^{2i}; \quad \text{where } \zeta = \frac{\Delta\sigma}{\sigma_0}, \quad (1)$$

σ_0 is the mean stress, $\Delta\sigma$ is the stress amplitude (half of the peak to peak amplitude), t_f^{static} is the time to failure under a constant stress, σ_0 , and n is the stress corrosion susceptibility parameter. The assumptions used to obtain this result are:

1. Power law crack growth kinetics, namely:

$$\frac{dc}{dt} = AK_I^n, \quad (2)$$

where K_I is the stress intensity factor.

2. n is integer.

3. Sinusoidal stress profile:

$$\sigma(t) = \sigma_0 + \Delta\sigma \sin \omega t = \sigma_0(1 + \zeta \sin \omega t). \quad (3)$$

4. Large number of cycles to failure, *i.e.* $\omega t_f^{cyclic} \gg 1$.

If any of these assumptions are violated, it will usually mean that the time to failure must be calculated by numerical integration of the fatigue equations.

We have developed a simple numerical approach to determining the time to failure under static conditions that does not require any of the assumptions above to be made. It uses a general form for the crack growth kinetics:

$$\frac{dc}{dt} = V(K_I). \quad (4)$$

Elimination of c from this equation and from the well known fracture mechanics relation:

$$K_I = \sigma Y \sqrt{c}, \quad (5)$$

where Y is the crack shape parameter, gives:

$$dK_I = \frac{\sigma^2 Y^2 V}{2K_I} dt. \quad (6)$$

This can be converted to a finite difference equation:

$$\Delta K_I = \frac{\sigma^2 Y^2 V}{2K_I} \Delta t, \quad (7)$$

which can provide the basis for a simple numerical integration algorithm that can be used for any kinetics model, $V(K_I)$ (including the power law with non-integer n), and for any stress profile, $\sigma(t)$. However, in the experiments described in this

paper, the fiber is loaded by a stepper motor. $\sigma(t)$ can be idealized for such a stepper motor system as a sequence of periods of static stress that change at each step the motor takes – a continuous form for $\sigma(t)$ is approximated by a sequence of discrete steps. However, (7) can be used to accurately model the stepper motor loading. Δt is taken as the time between steps. The value of K_I is calculated for each step from the stress at the start of the step and the current crack length. The change in K_I is then calculated from (7), from which the new crack length is determined after the step at a time Δt later. The stepper motor moves to give a new stress at the start of the next step and the process is repeated until K_I exceeds K_{IC} , the critical stress intensity factor, at which time the specimen fails. The only restriction on this approach is that there must be a sufficiently large number of steps to failure to ensure that K_I does not change much during each step else the finite difference equation (7) is inaccurate. Sufficient accuracy is expected for ≥ 100 steps to failure. Another consideration is that this integration scheme will become computationally inefficient for a very large number of motor steps to failure. However, it has been successfully applied to $>10^6$ steps to failure with computation times on the order of seconds.

3. EXPERIMENTAL

Cyclic fatigue has been performed on 125 μm diameter fused silica optical fiber covered with a UV-curable acrylate coating of outer diameter 250 μm . Fibers were tested immersed in $25.0 \pm 0.5^\circ\text{C}$ distilled water after preconditioning in the water for at least 24 hours. The fibers were broken using a two-point bending technique¹¹ in which the fiber is supported between grooved faceplates. The faceplates are moved by a stepper motor driven precision translation stage with an absolute positioning error of less than approximately $\pm 10 \mu\text{m}$ from all sources (zero offset, non-linearity, backlash, etc.). The resolution of the translation stage is 1 μm per step. The motor is controlled by a computer which times the steps to a precision of $\pm 50 \mu\text{s}$. The computer was programmed to give an inscribed piece-wise approximation to a sinusoidal variation in applied stress. These specifications mean that the stress at any given time is well within an error of 1% for the entire duration of the experiment. This precision control would be extremely difficult to achieve using other commonly used loading techniques, such as uniaxial tension.

The relationship between faceplate separation, d , and stress on the fiber is non-linear:

$$d = \frac{Ed_f}{\sigma(t)} - 2d_g + d_c = \frac{Ed_f}{\sigma_0} \frac{1}{(1 - \zeta \cos \omega t)} - 2d_g + d_c, \quad (8)$$

Where d_f and d_c are the glass and coating diameters, d_g is the depth of the grooves in the faceplates and E is the Young's modulus of the glass. Therefore the faceplate speed and acceleration do not vary sinusoidally with time for a sinusoidal variation in stress (3):

$$\dot{d} = -\frac{Ed_f}{\sigma_0} \zeta \omega \frac{\sin \omega t}{(1 - \zeta \cos \omega t)^2}, \quad (9)$$

$$\ddot{d} = -\frac{Ed_f}{\sigma_0} \zeta \omega^2 \frac{-2\zeta + \cos \omega t + \zeta \cos^2 \omega t}{(1 - \zeta \cos \omega t)^3}. \quad (10)$$

However, the computer program can readily calculate the necessary stepping profile for a sinusoidal or any other stress profile.

4. RESULTS

Figure 1 shows experimental results for a mean stress of $\sigma_0 = 4300 \text{ MPa}$ and for frequencies in the range of 0 to 100 Hz. Also shown are the predictions of the Evans and Fuller model,² (1), for $n = 20$. The numerical integration scheme has been used to predict the behavior using the power law (2) for frequencies of 1 and 10 Hz. The 10 Hz result is indistinguishable from the Evans and Fuller model, thus validating the accuracy of the integration algorithm. The agreement between these curves and the data is close for all frequencies, indicating no cyclic effects over and above subcritical crack growth.

At the lower frequency of 1 Hz, steps in the predicted behavior are observed at high stress amplitude. This behavior is expected because there is a small number of cycles to failure at this frequency – the Evans and Fuller model is inaccurate under these circumstances. The steps in the curve are caused by failures being clustered on the rising edge of the stress sine wave. This point is illustrated by the Weibull plot in Figure 2 which shows the distributions of failure times for a frequency of 0.3 Hz at four different stress amplitudes. The upper horizontal axis marks the times at which the stress is a maximum (after $\frac{1}{2}$, $1\frac{1}{2}$, $2\frac{1}{2}$ periods). The clustering close to these maxima is then apparent. It can be seen that, depending on

where the time to failure distribution lies compared to the maxima, either narrow or anomalously broad distributions can be observed. This explains the large variability in the error bars observed in Figure 1 at large stress amplitude. These results show that the integration scheme can successfully predict not only the mean time to failure, but also the shape of the time to failure distribution as well.

Figure 3 shows the data of Figure 1 regraphed as time to failure versus frequency for various stress amplitudes. The failure times do not show any systematic trend with frequency. Therefore, at least in the frequency range considered, the fatigue is frequency independent, again indicating that there are no additional cyclic effects.

Figure 4 shows the time to failure as a function of amplitude for mean stresses of 3900 and 4300 MPa. Figure 4(a) shows that the behavior for 3900 MPa can be predicted from the behavior at 4300 MPa using the numerical integration scheme and a value of $n = 20$. This means that when the failure times are normalized to the time to failure under static conditions, Figure 4(b), the data all lie on one master curve.

The numerical integration scheme has been used to fit other kinetics models besides the empirical power law (Eq. 2), designated model 1. Two other kinetic forms that are based on chemical kinetics models have also been fitted, namely model 2:¹²

$$\frac{dc}{dt} = A' \exp(n'K_I), \quad (11)$$

and model 3:¹²

$$\frac{dc}{dt} = A'' \exp(n''K_I^2). \quad (12)$$

The results of the fitting are shown in Figure 5. All three models provide a good fit to the data and so the data can not be used to distinguish the most appropriate kinetic form. The three models show the same trends at lower amplitude but their predictions diverge for $\zeta \geq 0.2$. In on going research we are making a more extensive investigation at higher amplitudes in order to provide evidence to distinguish between the models. It is important to know which form is most appropriate since lifetime predictions are sensitive to this form. In particular, the empirical power law predicts longer lifetimes than the exponential forms^{13,12} and is therefore not as conservative.

5. CONCLUSIONS

The two-point bending technique has been used to investigate the cyclic fatigue behavior of high strength fused silica optical fiber. The results agree well with the predictions of the subcritical crack growth model for fatigue. In particular, the results are found to be independent of the frequency of the cyclic component of stress up to 100 Hz. These results indicate that, at least in the range of stress and frequency studied here, there are no additional cyclic fatigue effects over and above subcritical crack growth.

A numerical integration scheme has been developed that accurately models the stress history in the two-point bend apparatus when driven by a stepper motor. This integration scheme avoids the limitations of the closed form result of Evans and Fuller.² The scheme has been used to fit several different crack growth kinetics models to the experimental data. It is shown that extensive cyclic fatigue data have the potential to distinguish between these models. It is noted that predicted lifetime of optical fiber is sensitive to the form of the kinetics model.

While the results of this and earlier work indicate that the cyclic fatigue behavior can be explained solely in terms of subcritical crack growth, the results are for moderate frequencies and relatively short failure times. These results therefore do not preclude the possibility of additional cyclic effects that might only become apparent after a very large number of stress cycles, *i.e.* for higher frequencies and long times to failure. Further work is needed to establish definitively whether cyclic fatigue causes increased degradation.

6. REFERENCES

1. J. B. Wachtman, *Mechanical Properties of Ceramics*, Wiley, New York, NY, 1996.
2. A. G. Evans and E. R. Fuller, "Crack propagation in ceramic materials under cyclic loading conditions," *Met. Trans.*, **5** 27-33 1974.

3. A. G. Evans and M. Linzer, "High frequency cyclic crack propagation in ceramic materials," *Int. J. Fracture*, **12** [2] 217-222 1976.
4. S. J. Dill, S. J. Bennison and R. H. Dauskardt, "Subcritical crack-growth behavior of borosilicate glass under cyclic loads: evidence of a mechanical fatigue effect," *J. Am. Ceram. Soc.*, **80** [3] 773-776 1997.
5. J. A. Wysocki, M. N. Colborn, S. N. Alam and J. R. Varner, "Low cycle fatigue behavior of metal-coated silica fibers," *J. Non-Cryst. Solids*, **42** 261-268 1980.
6. H. N. Rogers, "Cyclic fatigue behavior of silica fiber," *Proc. Soc. Photo-Opt. Instrum. Eng.*, **1366** 112-117 1990.
7. Y. Katsuyama, Y. Mitsunaga, H. Kobayashi and Y. Ishida, "Dynamic fatigue of optical fiber under repeated stress," *J. Appl. Phys.*, **53** [1] 318-321 1982.
8. P. Mauron, P. M. Nellen, U. Sennhauser, M. N. Trutzel, D. Betz, L. Staudigel, V. Hagemann and M. Rothhardt, "Lifetime of fibre Bragg gratings under cyclic fatigue," *Proc. Soc. Photo-Opt. Instrum. Eng.*, **3848** 212-220 1999.
9. P. Mauron, P. M. Nellen and U. Sennhauser, "Cyclic loading of optical fibres," *Proc. EuroCable Conf. '99*, 1999.
10. E. R. Roneree, V. L. Thomas and M. J. Matthewson, "Effect of loading scheme on the fatigue behavior of fused silica optical fiber," abstract in *Bull. Am. Ceram. Soc.* **74** 294 1995.
11. M. J. Matthewson, C. R. Kurkjian and S. T. Gulati, "Strength measurement of optical fibers by bending," *J. Am. Ceram. Soc.*, **69** [11] 815-821 1986.
12. M. J. Matthewson, "Chemical kinetics models for the fatigue behavior of fused silica optical fiber," *Mat. Res. Soc. Symp. Proc.*, **531** 143-153 1998.
13. K. Jakus, J. E. Ritter, Jr. and J. M. Sullivan, "Dependency of fatigue predictions on the form of the crack velocity equation," *J. Am. Ceram. Soc.*, **64** [6] 372-374 1981.

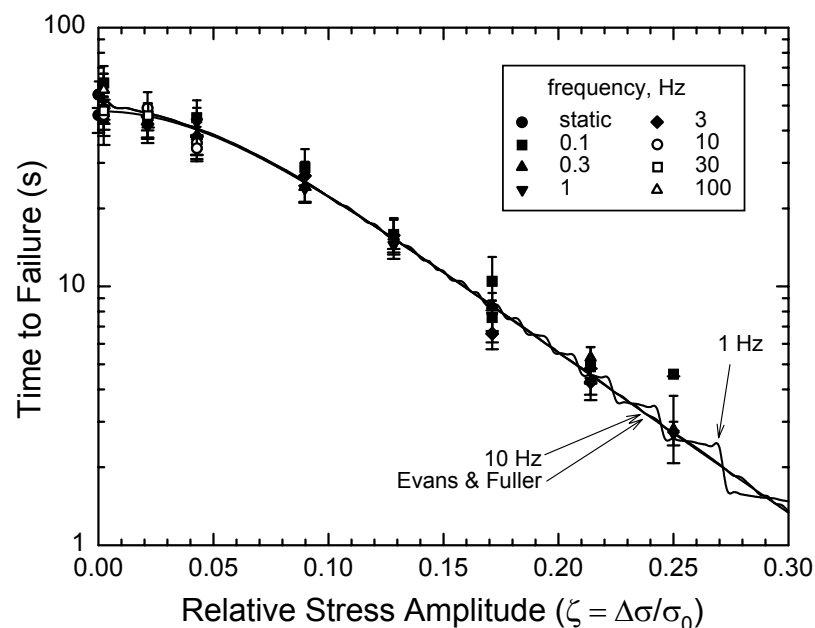


Figure 1. Time to failure under cyclic fatigue as a function of stress amplitude, ζ , for a mean stress of $\sigma_0 = 4300$ MPa. Data are for frequencies ranging from 0 to 100 Hz.

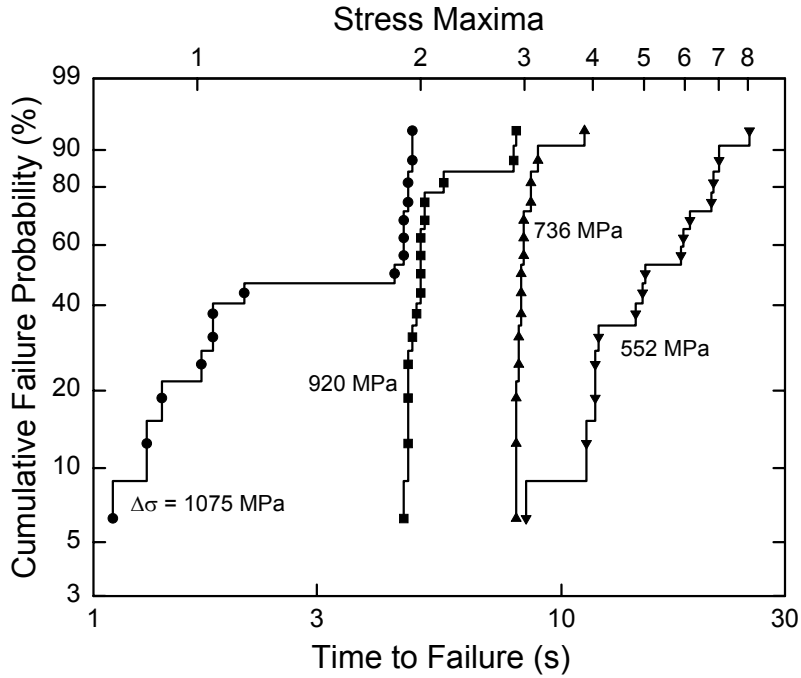


Figure 2. Weibull distributions for the time to failure for a mean stress of $\sigma_0 = 4300$ MPa and frequency 0.3 Hz for stress amplitudes, $\Delta\sigma = 552, 736, 920$ and 1075 MPa.

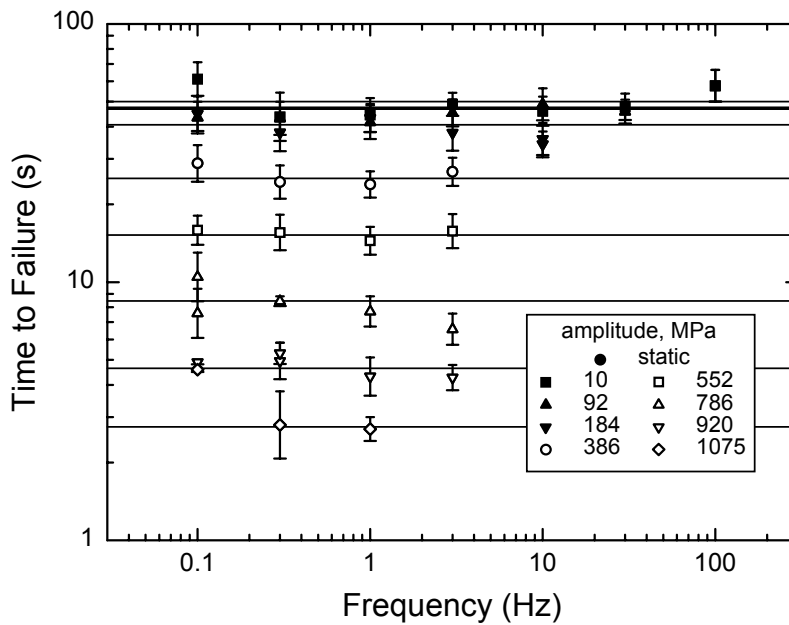


Figure 3. Data from Figure 1 regraphed as a function of frequency. $\sigma_0 = 4300$ MPa.

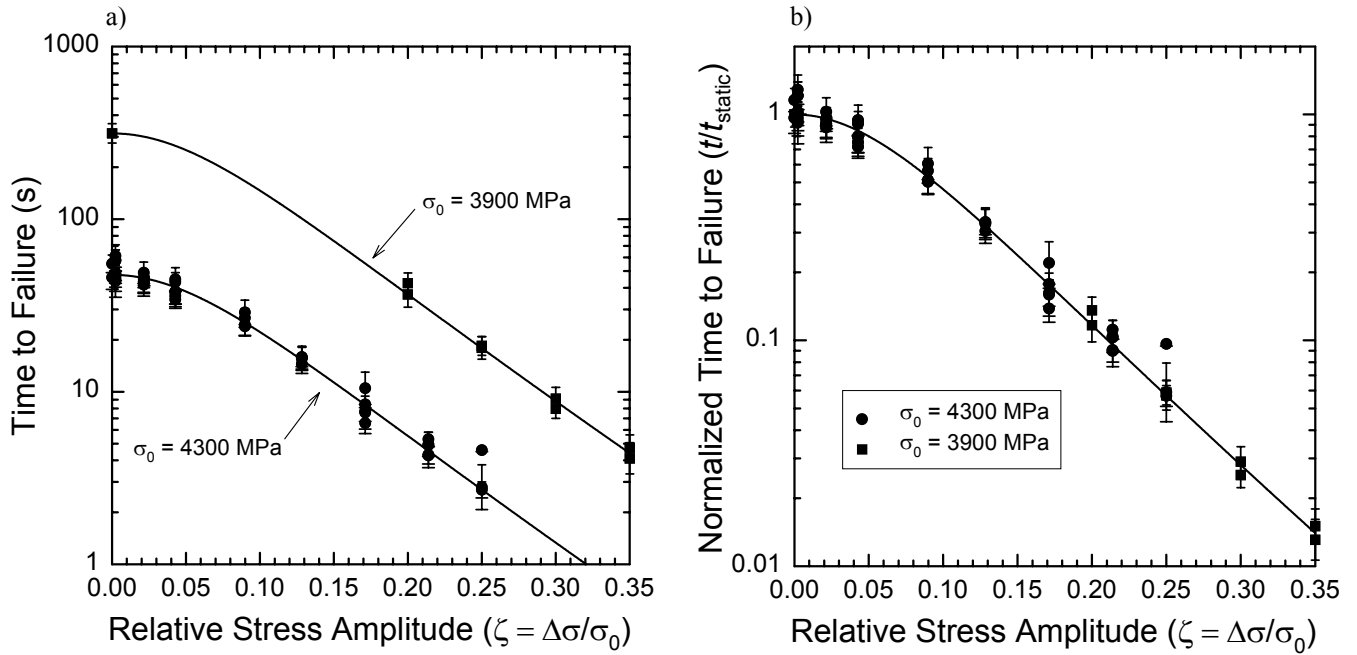


Figure 4. (a) time to failure and (b) time to failure normalized to the static failure time, as a function of stress amplitude for mean stresses, σ_0 , of 3900 and 4300 MPa. Prediction lines are calculated for $n = 20$.

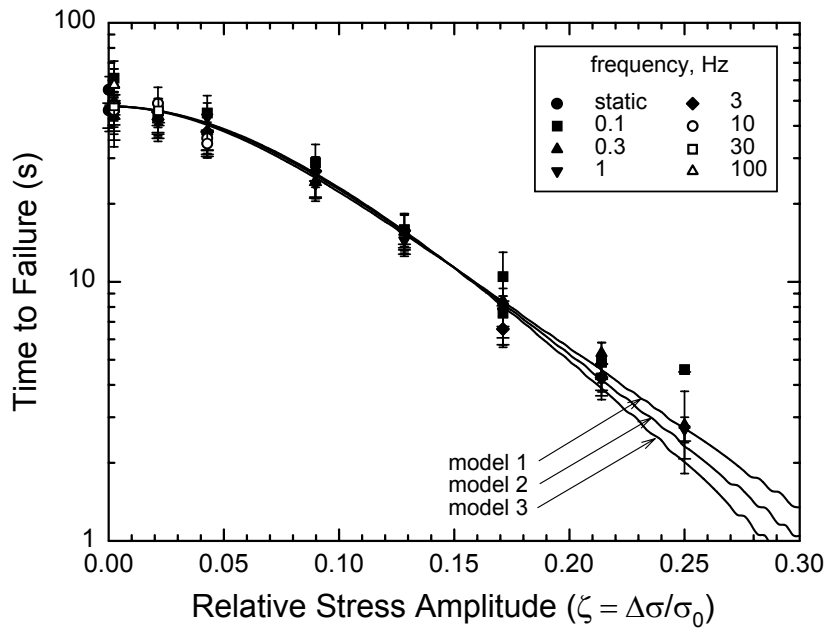


Figure 5. Three forms of the crack growth kinetics model fitted to the data of Figure 1.